WL-TR-90-53

WL-TR-
90-53

AD-A231 274

(2)

A NUMERICAL SOLUTION SCHEME FOR SOFTENING PROBLEMS INVOLVING TOTAL STRAIN CONTROL

Z. Chen
H. L. Schreyer

New Mexico Engineering Research Institute
University of New Mexico
Albuquerque, NM 87131

October 1990

Final Report

Approved for public release; distribution unlimited.

Weapons Laboratory
Air Force Systems Command
Kirtland Air Force Base, NM 87117-6008

This final report was prepared by New Mexico Engineering Research Institute, Albuquerque, New Mexico, under Contract F29601-84-C-0080, Job Order 2302Y207, with the Weapons Laboratory, Kirtland Air Force Base, New Mexico. Major John J. Gill (NTES) was the Laboratory Project Officer-in-Charge.

This technical report has been reviewed and is approved for publication.

John J. Gill

JOHN J. GILL
Maj, USAF
Project Officer

FOR THE COMMANDER

Thomas E. Bretz

THOMAS E. BRETZ, JR
Lt Col, USAF
Chief, Civil Engr Rsch Div

George Y. Baladi

GEORGE Y BALADI
Technical Advisor
Civil Engr Rsch Div

REPORT DOCUMENTATION PAGE

Form Approved
OMB No. 0704-0188

1. AGENCY USE ONLY *(Leave blank)*

2. REPORT DATE
October 1990

3. REPORT TYPE AND DATES COVERED
Final Dec 88 - Sep 89

4. TITLE AND SUBTITLE
A NUMERICAL SOLUTION SCHEME FOR SOFTENING PROBLEMS INVOLVING TOTAL STRAIN CONTROL

5. FUNDING NUMBERS
PE: 63231F
PR: 2302
TA: Y2
WU: 07

6. AUTHOR(S)
Z. Chen and H. L. Schreyer

7. PERFORMING ORGANIZATION NAME(S) AND ADDRESS(ES)
New Mexico Engineering Research Institute
University of New Mexico
Albuquerque, New Mexico 87131

8. PERFORMING ORGANIZATION REPORT NUMBER
SS 6101(2)

9. SPONSORING/MONITORING AGENCY NAME(S) AND ADDRESS(ES)
Weapons Laboratory
Kirtland AFB, NM 87117-6008

10. SPONSORING/MONITORING AGENCY REPORT NUMBER
WL-TR-90-53

11. SUPPLEMENTARY NOTES

12a. DISTRIBUTION/AVAILABILITY STATEMENT
Approved for public release; distribution is unlimited

12b. DISTRIBUTION CODE

13. ABSTRACT *(Maximum 200 words)*
Nonlinear structural problems in which material softening is present constitute a severe challenge to solution algorithms. Most of the existing computational codes are based on using an incremental procedure with iterations and suitable constraints. Among the types of constraints are load control, direct or indirect displacement control, and arc-length control involving a combination of load and displacement paramenters. For many problems in which softening and localization occur, these algorithms fail at some point in the post-peak regime. In an attempt to remedy this problem, an alternative constraint condition is proposed whereby a combination of the total strain components is prescribed at the most critical point in the body. The critical point is defined to be that point where a suitable measure of strain is a maximum. Numerical solutions for both plane strain and plane stress problems are given to illustrate the ability of the procedure to capture post-peak responses of structures governed by materially nonlinear behavior.

14. SUBJECT TERMS

Penetration	Cap	Hydrostat
Nonlinear Finite Element Method	Coulomb	Hydrostatic
Prager-Drucker	Ogival	Dry Granular Soils

15. NUMBER OF PAGES
40

16. PRICE CODE

17. SECURITY CLASSIFICATION OF REPORT	18. SECURITY CLASSIFICATION OF THIS PAGE	19. SECURITY CLASSIFICATION OF ABSTRACT	20. LIMITATION OF ABSTRACT
Unclassified	Unclassified	Unclassified	

PREFACE

This research effort was conducted under the auspices of the Air Force Office of Scientific Research. Specifically, this research was designated as task 2302Y204 and is the result of the joint efforts of Weapons Laboratory Civil Engineering Research Division personnel (Geologic Response Section) and research scientists of the New Mexico Engineering Research Institute (NMERI). Their work was accomplished under contract F29601-84-0080. The technical effort was conducted between February and December 1988 with the final report being published in June 1989.

The support of this work by the Air Force Office of Scientific Research is gratefully acknowledged.

This effort was conducted under the technical supervision of Captain John Gill, Ph.D. Technical editing was performed by Dr. George Baladi, Ph.D., PE; Lt. Col. Thomas E. Bretz, Jr.; Captain Jay Logan; and Captain John J. Gill.

CONTENTS

ILLUSTRATIONS

1.0 INTRODUCTION

Nonlinear structural analyses include materially nonlinear problems such as nonlinear constitutive equations with small deformations, geometrically nonlinear problems normally associated with buckling, or a combination of both types of nonlinearities (1). If the tangent stiffness matrix, $\mathbf{K}$, is defined to include both types of nonlinearities, a limit or bifurcation point is characterized by a critical state at which the tangent stiffness matrix satisfies the static stability criterion

$$\mathbf{K}^c \Delta \mathbf{u}^c = \mathbf{0} \tag{1-1}$$

in which $\Delta \mathbf{u}^c$ denotes the vector (eigenmode) of displacement increments. Solutions for the displacement vector beyond critical points are important for describing the failure process and for making comparisons with experimental data (2, 3).

Most solution schemes for nonlinear problems are based on step-by-step load incrementation and an iteration procedure to correct for the linearization error. To trace nonlinear response beyond critical points, several methods have been proposed to circumvent the singularity that appears in the tangent stiffness matrix. One method is to detect the presence of negative pivots from the decomposition of $\mathbf{K}^c$ and then replace $\mathbf{K}^c$ with an expression of the type $\mathbf{K}^c + \eta\mathbf{I}$ with $\eta > 0$ so that this matrix is "safely" positive definite in the vicinity of critical points (4). A second method consists of suppressing the iterations around the critical point and reversing the sign of the load following the appearance of the negative pivot (5, 6). In order to avoid deviating too far from the equilibrium path, very small load steps have to be used in the range where no iterations are performed. Because it is extremely difficult to obtain converged solutions around critical points by simply prescribing external load increments, it has been suggested that the load level become a function of another variable. Direct displacement control (7), arc-length control (8), self-adaptive "hyperelastic" constraints (9), and indirect displacement control (10) are designed to provide such a constraint function through which the load level changes from iteration to iteration. For the case of snap-through in geometrically nonlinear problems, direct displacement control fails and arc-length control appears to be a robust procedure. However, for materially nonlinear analyses, a global norm on incremental displacements as used in arc-control is often less successful due to localization effects, and it may be more appropriate to employ only one dominant degree of freedom or to omit some degrees of freedom from the norm of incremental displacements. Such a scheme is often referred to as one of "indirect displacement control." The disadvantage of modifying the constraint condition is that the constraint function becomes problem dependent.

Recently, with the increase in interest in softening which is accompanied by localization, the need for a robust solution strategy has become of paramount importance. Efforts have been made towards modifying arc-length control so that the constraint equation is sensitive to the change of state variables within the localization zone. One modification is to use the eigenvector of the lowest eigenvalue of the tangent stiffness matrix as a trigger to move the solution from the unstable, unlocalized path (11, 12). Another one is the minimization of a function of an out-of-balance force vector to seek a dominant direction and a line search procedure along that direction (4). The line search method improves the convergence characteristics of arc-length control by introducing a variable step-length parameter, which scales the usual iterative displacement vector (13). Since these solution strategies have not been applied routinely to multidimensional problems involving general constitutive equations, they must be considered as tentative measures in the search for a general robust scheme. A better mathematical foundation is required for the application of line search techniques when tracing unstable equilibrium paths, and the issue of appropriate incremental quantities needs further consideration. It has been pointed out that existing procedures will not eliminate the difficulties associated with the dependence on increment sizes and on alternative equilibrium states, although nonlocal constitutive models may reduce the mesh-dependency of numerical solutions (11).

In general, arc-length control is still commonly used in geometrically nonlinear problems and, with some modifications, in materially nonlinear analyses since arc-length control can trace the post-peak response even for snap-through and snap-back problems. Occasionally, lack of convergence is reported even after the limit or bifurcation point has been traversed. One reason might be due to the fact that the load increment in the first iteration has to be prescribed according to some condition, and there is a sign change of the load increment during the transition from the pre-peak to the post-peak regimes. The choice of sign proves to be very important in calculations, and guidelines for sign change are discussed by Crisfield (5). The basic idea is that the sign of the load increment follows that of the previous increment unless the determinant of the tangent stiffness matrix changes sign, in which case a sign reversal is applied to the load increment. Usually, the $\mathbf{L}\text{-}\mathbf{D}\text{-}\mathbf{L}^T$ decomposition is used to factor the tangent stiffness matrix. The determinant of $\mathbf{K}^c$ is equal to the determinant of the diagonal matrix, $\mathbf{D}$, and the appearance of negative eigenvalues corresponds to the appearance of negative pivots in the decomposition. Since more than one negative pivot may appear simultaneously, the sign of each pivot, and not the product of the pivots, must be monitored to detect the appearance of negative eigenvalues. Unfortunately, numerical calculations involve finite digit arithmetic, and if the pivots are small, slight perturbations may produce large numerical errors (14). Therefore, an incorrect conclusion may be inferred with respect to the sign of the load increment, and the iterative procedure may not converge.

To circumvent some of these difficulties, and to accommodate the physical feature that softening is accompanied by localization, an alternative constraint approach is proposed that automatically yields the appropriate load increment. With the use of a suitable measure of strain, the point in the body with the maximum value of this measure is located at each load step, and an increment in a combination of the strain components at this point is prescribed. The resulting equations represent a slight extension to those used previously by Crisfield, de Borst, and their co-workers (5, 10). However, as illustrated through the solution to model problems in plane strain and plane stress, such a modification appears to result in a solution scheme from which the complete post-peak regime is easily obtained.

2.0 THEORETICAL FORMULATION

Consider a spatially discretized system based on the finite element method in which the vector of nodal displacements is denoted by $\mathbf{u}$ and an increment by $\Delta\mathbf{u}$. With a superscript defining the element, the incremental strain-nodal displacement relation over an element is given by

$$\Delta\mathbf{e}^e = \mathbf{B}^e\Delta\mathbf{u}^e \tag{2-1}$$

in which $\mathbf{e}$ denotes the strain vector and $\mathbf{B}$ relates the strain and nodal displacement components through a differential operator and interpolation functions. If s denotes the stress vector and C the continuum tangent stiffness, then the incremental relation between stress and strain is

$$\Delta\mathbf{s} = \mathrm{C}:\Delta\mathbf{e} \tag{2-2}$$

If R^e represents the domain of an element, then the element tangent stiffness matrix is

$$\mathbf{K}^e = \int_{R^e} \mathbf{B}^{e^T}\,\mathrm{C}\,\mathbf{B}^e\,dV \tag{2-3}$$

in which dV denotes the volume element. The global tangent stiffness matrix, $\mathbf{K}$, is obtained through a sum of the element contributions.

Only proportional loading will be considered; then the load vector is given by $\mu\mathbf{q}$ in which $\mathbf{q}$ is fixed and μ represents the magnitude of the load. For nonlinear problems $\mathbf{K}$ depends on $\mathbf{u}$ from geometrical and material nonlinearities of which only the latter will be considered. One method for obtaining solutions is to solve the incremental equilibrium relation

$$\mathbf{K}\,\Delta\mathbf{u} = \Delta\mu\mathbf{q} \tag{2-4}$$

in which $\Delta\mu$ is given and

$$\mu = \mu^P + \Delta\mu \qquad \mathbf{u} = \mathbf{u}^P + \Delta\mathbf{u} \qquad \mathbf{K} = \mathbf{K}(\mathbf{u}) \tag{2-5}$$

The superscript p denotes the variable at the end of the previous incremental step. Because the updated stiffness matrix is not known, an iterative procedure is required to obtain a solution. If I is used as the iteration count, and with $\mathbf{u}_0 = \mathbf{u}^p$, one approach is to solve iteratively

$$\mathbf{K}_{I-1}\delta\mathbf{u}_I = \Delta\mu\mathbf{q} \qquad \mathbf{u}_I = \mathbf{u}_{I-1} + \delta\mathbf{u}_I \qquad \mathbf{K}_{I-1} = \mathbf{K}(\mathbf{u}_{I-1}) \tag{2-6}$$

until a convergence criterion is met. However, for problems in which a limit load and softening are expected, $\Delta\mu$ cannot be prescribed and, instead, must be determined indirectly as part of the iterative solution procedure. To remove the resulting indeterminacy, a combination of displacement components and load increment is often prescribed in an "arc control" method, which permits a solution to be obtained even if the tangent stiffness matrix contains zero or negative eigenvalues. If this constraint is left open for the moment, such procedures are obtained by recasting (2-6) in the form

$$\begin{gathered}\mathbf{K}_{I-1}\delta\mathbf{u}_I = \delta\mu_I\mathbf{q} + \mathbf{r}_{I-1} \qquad \mathbf{r}_{I-1} = \mu_{I-1}\mathbf{q} - \int_R \mathbf{B}^T\mathbf{s}_{I-1}dV \\ \mu_I = \mu_{I-1} + \delta\mu_I \qquad \mu_0 = \mu^p\end{gathered} \tag{2-7}$$

in which the residual $\mathbf{r}_{I-1}$ is included to prevent incremental drifting away from the equilibrium state. This equation is identical to that derived by de Borst (10), but with a different point of view. However, an alternative form of (2-7) is more common. Let

$$\mathbf{p}_I = \mu_0\mathbf{q} - \int_R \mathbf{B}^T\mathbf{s}_{I-1}dV \tag{2-8}$$

Then (2-7) becomes

$$\mathbf{K}_{I-1}\delta\mathbf{u}_I = \Delta\mu_I\mathbf{q} + \mathbf{p}_{I-1} \qquad \mu_I = \mu_0 + \Delta\mu_I \tag{2-9}$$

At this stage the subincrement in the solution vector is considered to be the sum of two parts:

$$\delta \mathbf{u}_I = \Delta\mu_I \delta \mathbf{u}_I^q + \delta \mathbf{u}_I^p \qquad \Delta \mathbf{u}_I = \Delta \mathbf{u}_{I-1} + \delta \mathbf{u}_I \qquad \Delta \mathbf{u}_0 = \mathbf{0}$$

$$\mathbf{K}_{I-1} \delta \mathbf{u}_I^q = \mathbf{q} \qquad \mathbf{K}_{I-1} \delta \mathbf{u}_I^p = \mathbf{p}_{I-1} \tag{2-10}$$

With this formulation the proposed method involving total strain control and its relationship to existing methods can be conveniently described. Conventional arc control methods specify the load increment in terms of global norms of displacement increments at the current iteration. Modified methods include contributions to the arc control of the increment in the displacement from the previous iteration. The basic point, however, is that global norms are used. For problems involving softening and localization, such norms may not be sensitive enough. Instead it is proposed here that a "localized" norm be used for this particular class of problem.

With the separation of the displacement increments into the parts given by (2-10), it follows from (2-1) that the increment in the strain vector for an element is

$$\Delta \mathbf{e}^e = \mathbf{B}^e \Delta \mathbf{u}^p + \Delta\mu \mathbf{B}^e \Delta \mathbf{u}^q \tag{2-11}$$

Suppose a linear combination of the increments in strain, Δe, is prescribed. Define an element constraint vector $\mathbf{c}^e$ such that

$$\Delta e = \mathbf{c}^{e^T} \Delta \mathbf{e}^e \tag{2-12}$$

Since $\Delta \mathbf{u}_I^p = \delta \mathbf{u}_I^p = \mathbf{0}$ for $I = 1$ if the convergence criterion is satisfied at the end of the previous increment, and since (2-12) is to be fixed throughout the load step, then the load increment, $\Delta\mu_I$, must satisfy the following equation:

$$\Delta\mu_I = \frac{\Delta e}{\mathbf{c}^{e^T}\mathbf{B}^e\delta\mathbf{u}_I^q} \qquad \text{for } I = 1$$

$$\Delta\mu_I = -\frac{\mathbf{c}^{e^T}\mathbf{B}^e\delta\mathbf{u}_I^p}{\mathbf{c}^{e^T}\mathbf{B}^e\delta\mathbf{u}_I^q} \qquad \text{for } I > 1 \tag{2-13}$$

For a general problem, it is logical to choose the governing element to which the constraint is to be applied as that element which has experienced the most distortion as reflected through a suitable norm of strain. For problems in which softening is a possibility, the critical element will be the one that first reaches the limit state, and this element is usually the one that continues to be critical because it softens the most. The use of (2-13), with the increment, Δe, always assumed to be of the same sign for consecutive load steps, avoids the difficulties associated with a singular tangent stiffness matrix at the limit load and with multiple negative eigenvalues in the post-peak regime. Rots (15) proposed a similar approach with a constraint condition involving the displacement components on either side of an active crack. However, he prescribes $\Delta\mu_1$ instead of the crack opening displacement in the first iteration. As a result there is a potential problem involving the monitoring of negative pivots for transitioning critical points. With the proposed approach involving total strain control, the sign and magnitude of $\Delta\mu_I$ are automatically adjusted throughout the iteration procedure.

With regard to a convergence criterion, the results of numerical investigations indicate that the energy criterion, which involves the product of the out-of-balance force with the increment in displacement, is not satisfactory, although a component of force may be large, the corresponding component of displacement increment is sufficiently small to cause the criterion to be satisfied. This situation arises frequently at limit points. Therefore, in the numerical examples of the next section, convergence is based on the following combined force and displacement criterion:

$$\frac{\|\boldsymbol{\delta u}_I\|}{\|\boldsymbol{\delta u}_1\|} \le \varepsilon_u$$

$$\frac{\|\Delta\mu_I \mathbf{q} + \mathbf{p}_{I-1}\|}{\|\Delta\mu_1 \mathbf{q} + \mathbf{p}_0\|} \le \varepsilon_\mu \tag{2-14}$$

where the 2-norm is inferred. This criterion is also used by Padovan and Tovichakchaikul (9). Although different values for the tolerances can be specified, for this study they were chosen to be $\varepsilon_u = \varepsilon_\mu = 0.001$. For most cases the part based on displacement is satisfied first.

3.0 NUMERICAL SOLUTIONS TO PLANE PROBLEMS

To illustrate the robustness of the proposed solution scheme, a simple bilinear hardening and softening model is used to simulate material behavior. The nonlocal aspect of post-peak response is not addressed and, therefore, post-peak solutions that depend on mesh size are to be expected.

The invariants of stress, $\bar{s}$, and plastic strain, $\bar{e}^p$, are defined in the usual manner from the deviators of stress, s^d and plastic strain, e^{pd}:

$$\bar{s} = \frac{3}{2}\mathrm{tr}\left(s^d \cdot s^d\right) \qquad \bar{e}^p = \int \frac{2}{3}\left(\mathrm{tr}\, de^{pd} \cdot de^{pd}\right) \tag{3-1}$$

The yield function is assumed to be

$$f = \frac{\bar{s} - H}{H_L} \tag{3-2}$$

in which H is a hardening-softening function and H_L denotes the limit, or maximum, value. With the definition

$$\bar{e}^* = \frac{\left(\bar{e}^p - \bar{e}^p_L\right)}{\bar{e}^p_L} \tag{3-3}$$

a bilinear relation for the hardening-softening function is conveniently described as follows:

$$\begin{aligned} &H = H_0 + (H_L - H_0)\frac{\bar{e}^p}{\bar{e}^p_L} && 0 \le \bar{e}^p < \bar{e}^p_L \\ &H = H_L(1 - m\,\bar{e}^*) && 0 \le \bar{e}^* < \frac{1}{m} \\ &H = 0 && \bar{e}^* \ge \frac{1}{m} \end{aligned} \tag{3-4}$$

in which H_0 denotes the elastic limit. The value of the plastic strain invariant at the limit state, $\bar{e}^p_L$, is assumed to be a unique value no matter which stress path is followed. The parameter, m, merely reflects the rate of softening. The yield and consistency conditions are given by f = 0 and df = 0, respectively. An associated flow rule is used. Normally, solutions to model problems in plane strain are given because the displacement formulation implies that the plane strain condition is satisfied easily. However, with the exception of some additional algebra involving the use of the tangent moduli, solutions to problems in plane stress can also be obtained for the same geometric configurations with little additional computational effort. Both classes of plane problems are considered next.

The geometry and notation for the plane problem is shown in Fig. 1. The dimensions used for the analysis are $L_x = 1$ m and $L_y = 1.5$ m. In order to accommodate isochoric deformation, the argument of Nagtegaal et al. (16) for the use of a four-node element composed of four triangles defined by the two diagonals in the quadrilateral is considered to be persuasive and, therefore, the same element is used in this study. The lateral surfaces are stress-free (except for plane strain) while the boundary condition at y = 0 consists of zero vertical displacement and a lateral constraint of zero displacement at one point which is x = 0 unless specified otherwise. The load is applied through a mechanism that provides no lateral constraint and ensures that the displacement in the y-direction is the same for all points on the upper surface. Since the plasticity model is that of von Mises, significant plastic deformations are exhibited in shear bands oriented at 45 deg to either coordinate. Another implication that follows from the use of the von Mises model is that the same results are obtained for loading in tension and compression so such a differentiation is not made in the subsequent description. Element mesh configurations I, II and III are defined to be 3 x 3, 5 x 7 and 9 x 13 rectangular grids, respectively.

In the elastic regime, the material is assumed to be isotropic as defined through Young's modulus, E, and Poisson's ratio, ν. Material parameters, which are considered to be representative of a class of geological materials, are chosen as follows (unless specified otherwise): E = 50 GPa, ν = 0.2, $\bar{e}^p_L = 0.011$, $H_0 = 0$, $H_L = 55$ MPa, and m = 0.1. The zero value for the elastic limit is chosen partly for convenience and partly so that unloading can be easily detected because the loading and unloading moduli are different right from the initiation of loading. Initial imperfections are introduced by letting $\bar{e}^p_L = 0.01$ and $H_L = 50$ MPa at a point in the body designated with the symbol ∇.

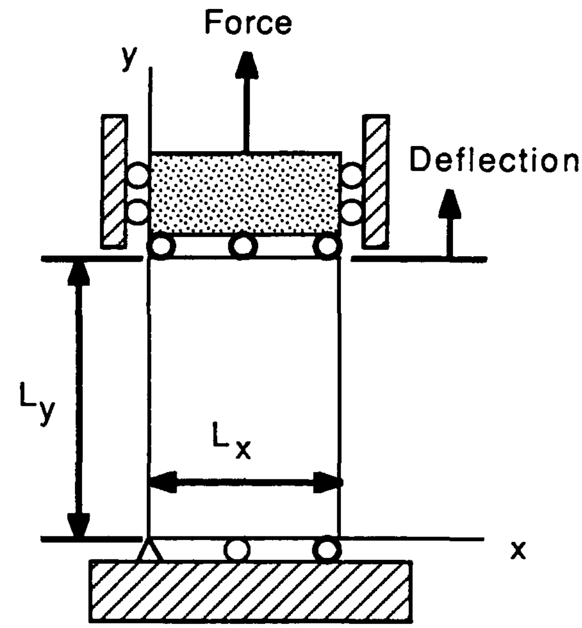

Figure 1. Geometry of the plane problem.

The first model problem is one of uniform loading in the y-direction under the assumption of plane strain (components with a subscript z are zero) with all components of displacement prescribed to be zero for the point at the origin. The constraint condition for the total strain increment in the critical element was chosen such that the increment in y-y component of normal strain is prescribed. The evolution of the deformation field for element configuration III is shown in Figs. 2(a) and 2(b) for plane strain. Because of the symmetrical location of the imperfections obtained by using an odd number of elements in each coordinate direction, two shear bands develop and intersect one end of the body. For the same mesh configuration and also for plane strain, Figs. 3, 4 , 5, and 6 show the failure modes that develop for different choices of the locations of initial imperfections and slightly different boundary conditions. The sensitivity of failure modes to imperfections and boundary conditions has been pointed out previously by Leroy et al. (17). For Figs. 3 and 4, the lateral constraint is at x = 0, while for Figs. 5 and 6 the constraint is at x = 1.0 and x = 0.5, respectively. Figure 3 shows crossed shear bands while Fig. 4 shows a single shear band that does not intersect either the top or bottom surface. Figure 5 is a mirror image of Fig. 4 because of the switch in location of the lateral constraint on the boundary. The symmetrical location of the lateral boundary constraint in Fig. 6 is reflected in a correspondingly symmetrical deformation field.

For plane stress and for the point at the origin fixed, Fig. 7 illustrates the corresponding final post-peak deformation field.

The effect of the size of the prescribed total strain increment for mesh configuration I is shown in Fig. 8 for plane strain. For the largest increment of 0.01 the peak load is achieved in only two steps so larger increments would not be meaningful. The fact that no signicant differences are displayed can probably be attributed to the use of a bilinear hardening-softening function.

For plane strain and for mesh configuration I, load-deflection curves are given in Fig. 9 for various values of the softening parameter. For m = 0.01, 0.1 and 1.0, the peak load per unit thickness and the corresponding deflections are (58.6 MN/m, 0.0171 m), (58.3 MN/m, 0.0160 m) and (52.8 MN/m, .0140 m), respectively. The loads and deflections shown in the figure are normalized with respect to these values.

For plane stress and also for mesh configuration I, Fig. 10 shows the effect of the softening parameter m on the load-deflection response. For m = 0.01, 0.1, and 1.0, the peak loads per unit thickness and the corresponding deflections are (56.1 MN/m, 0.0169 m), (55.7 MN/m, 0.0168 m) and (53.6 MN/m. 0.0150 m), respectively. As can be seen for both plane strain (Fig. 9) and plane stress (Fig. 10), numerical difficulties are not encountered for the full range of post-peak behavior

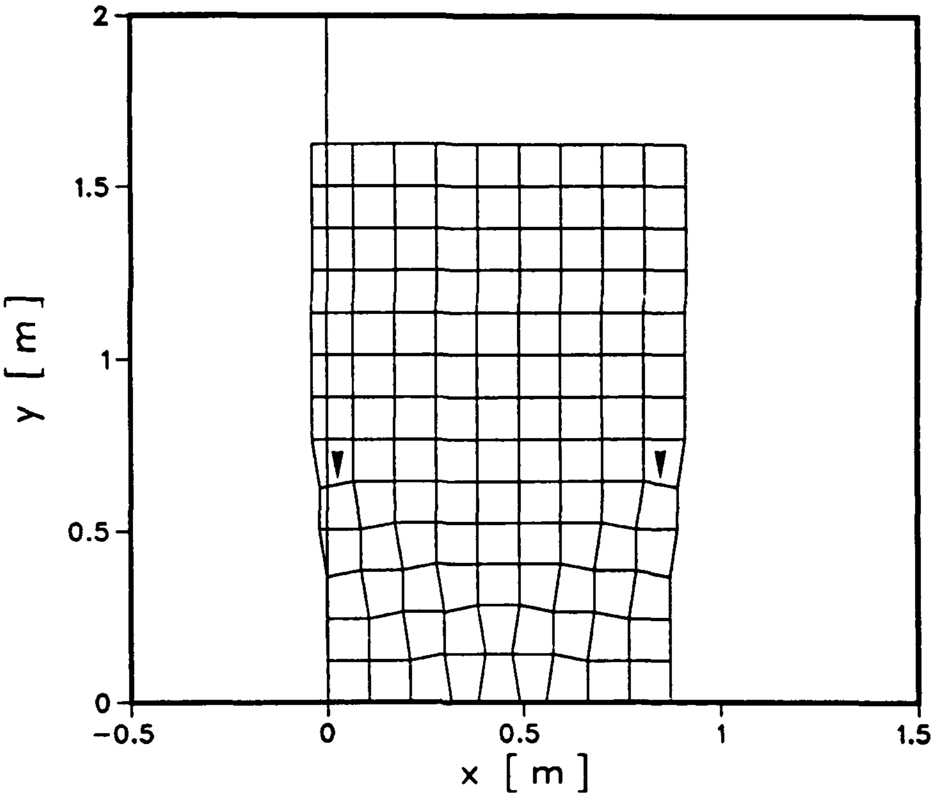

(a) Intermediate post-peak.

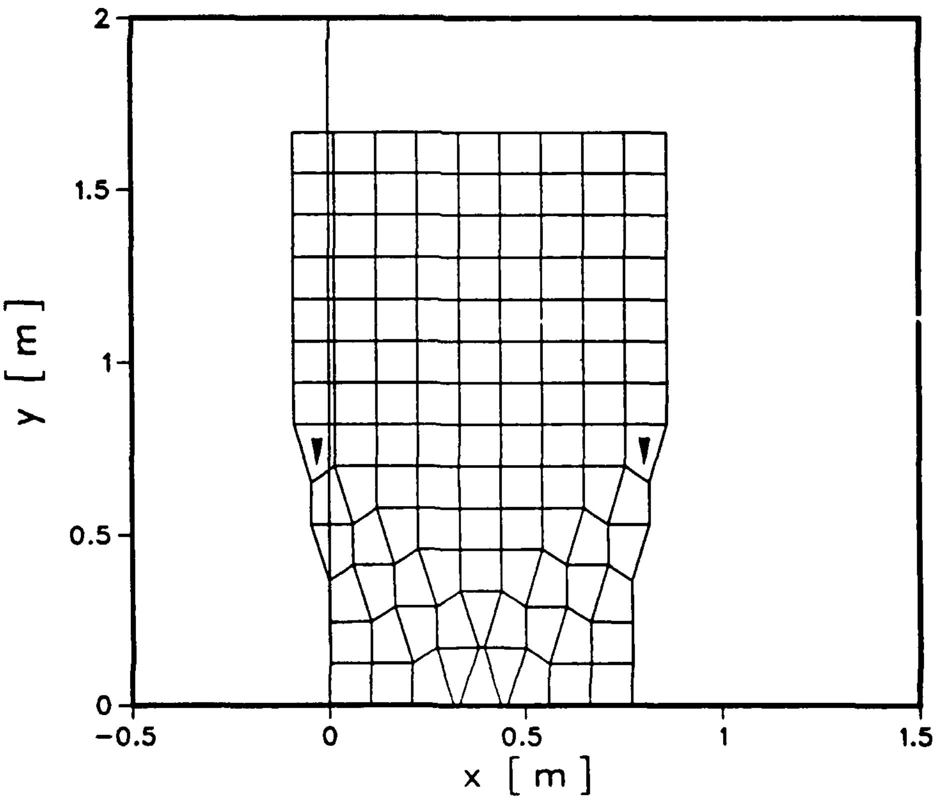

(b) Final post-peak.

Figure 2. Deformed mesh in the post-peak regime for plane strain and constraint at x = 0.

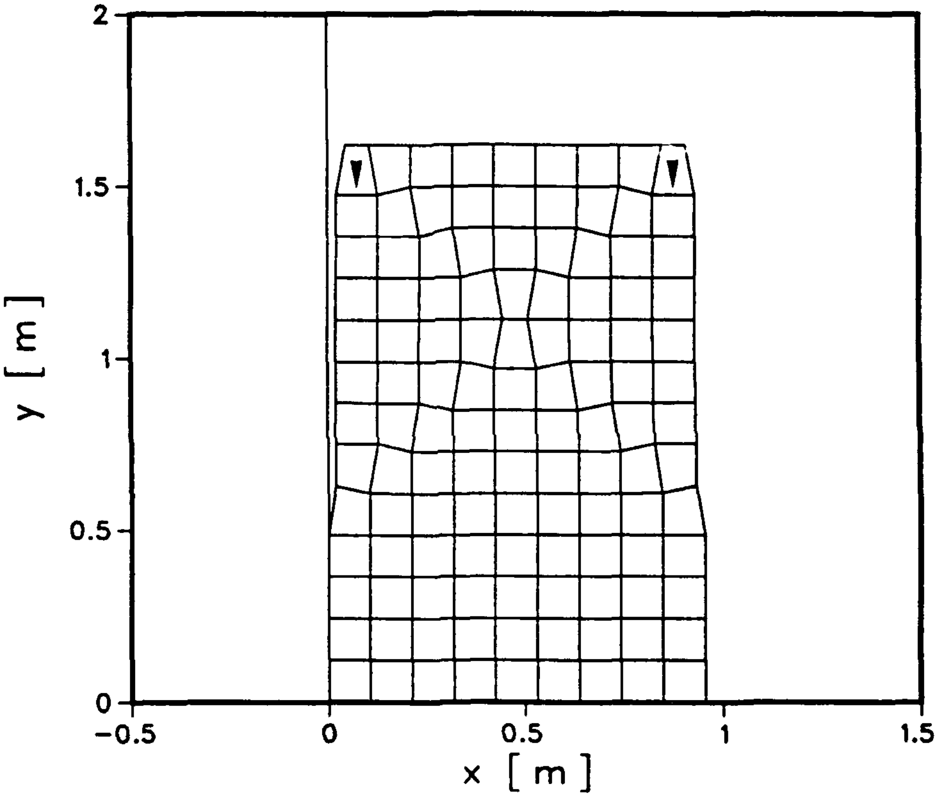

Figure 3. Final post-peak deformation field with two weak elements in the uppermost corners.

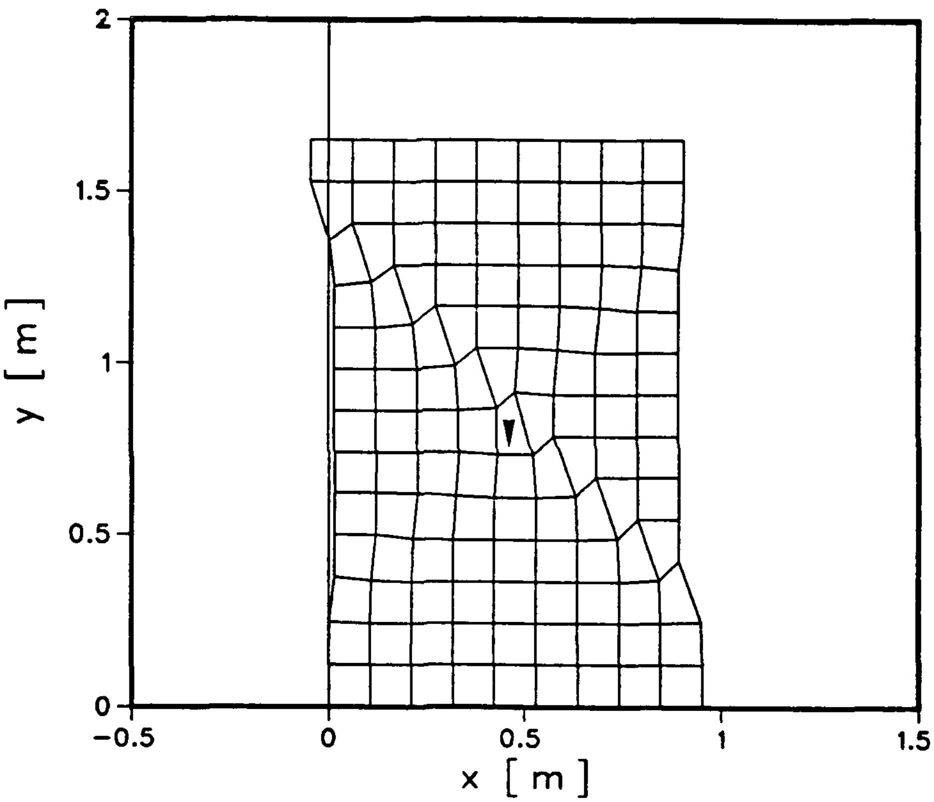

Figure 4. Final post-peak deformation field with the weak element at the center.

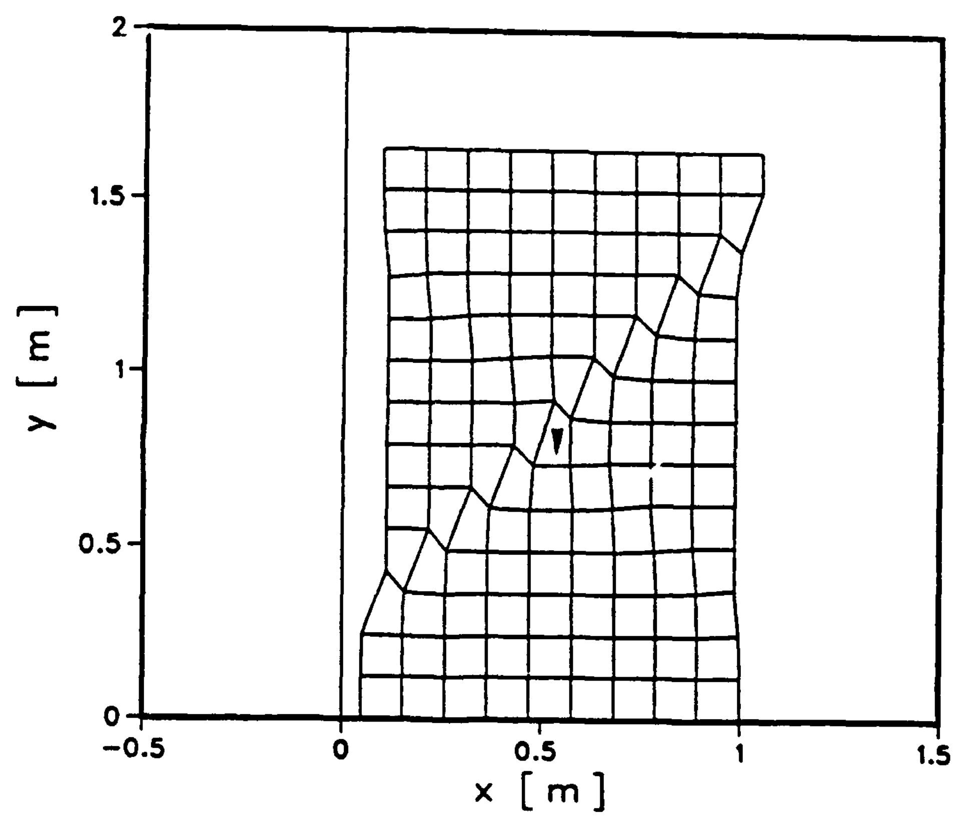

Figure 5. Final post-peak deformation field with constraint at x = 1.

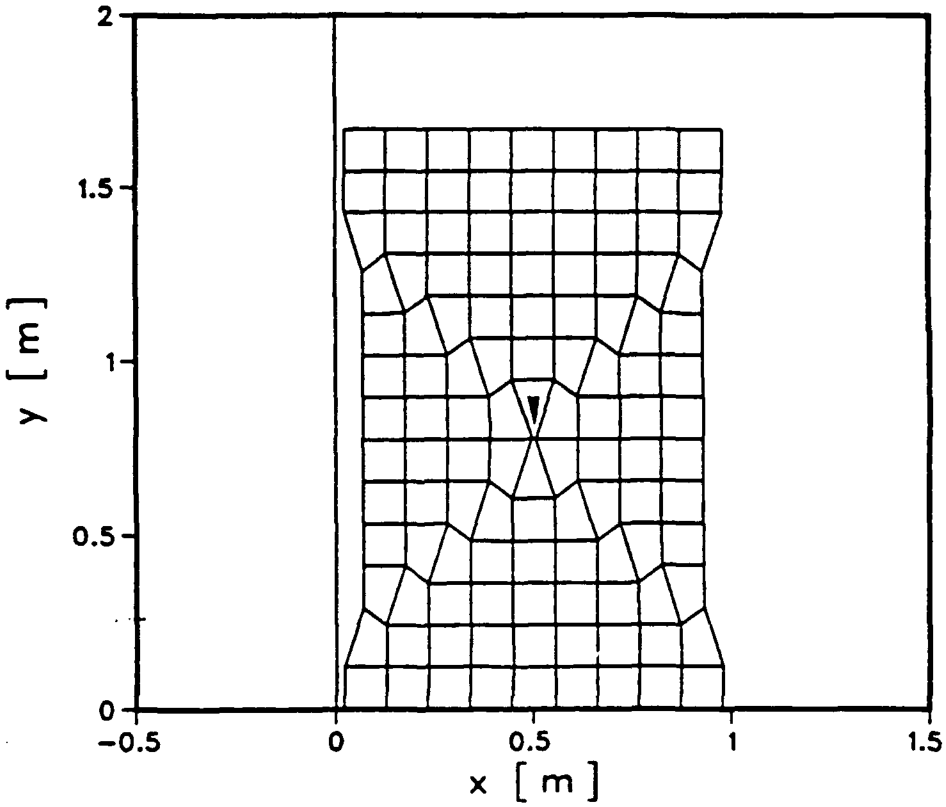

Figure 6. Final post-peak deformation field with constraint at x = 0.5.

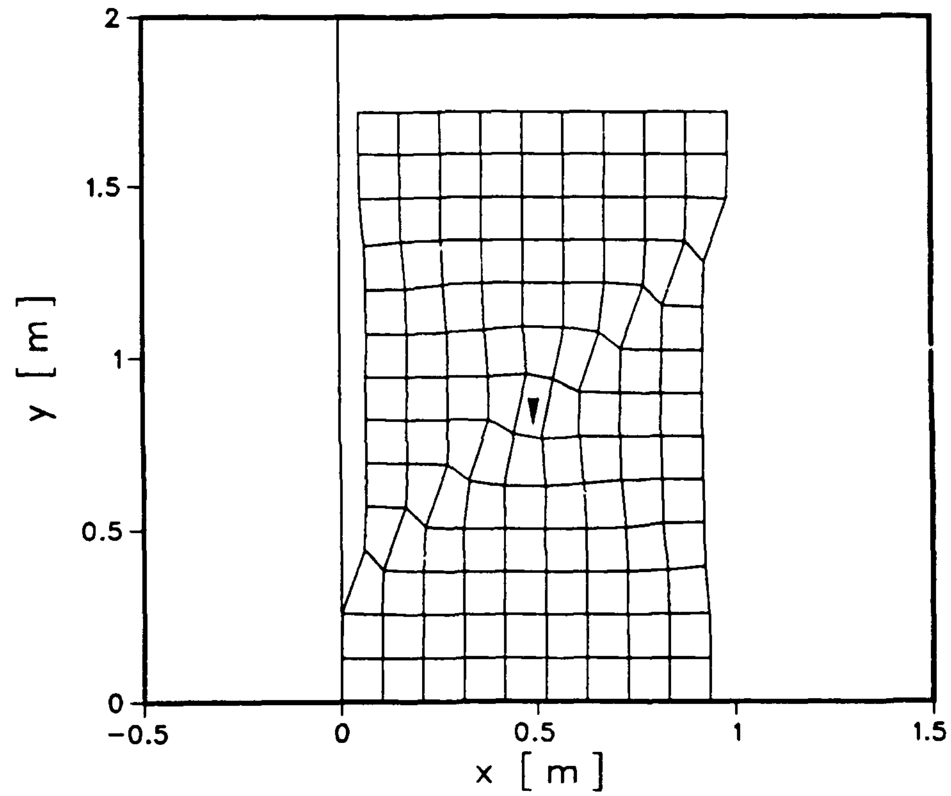

Figure 7. Final post-peak deformation field for plane stress.

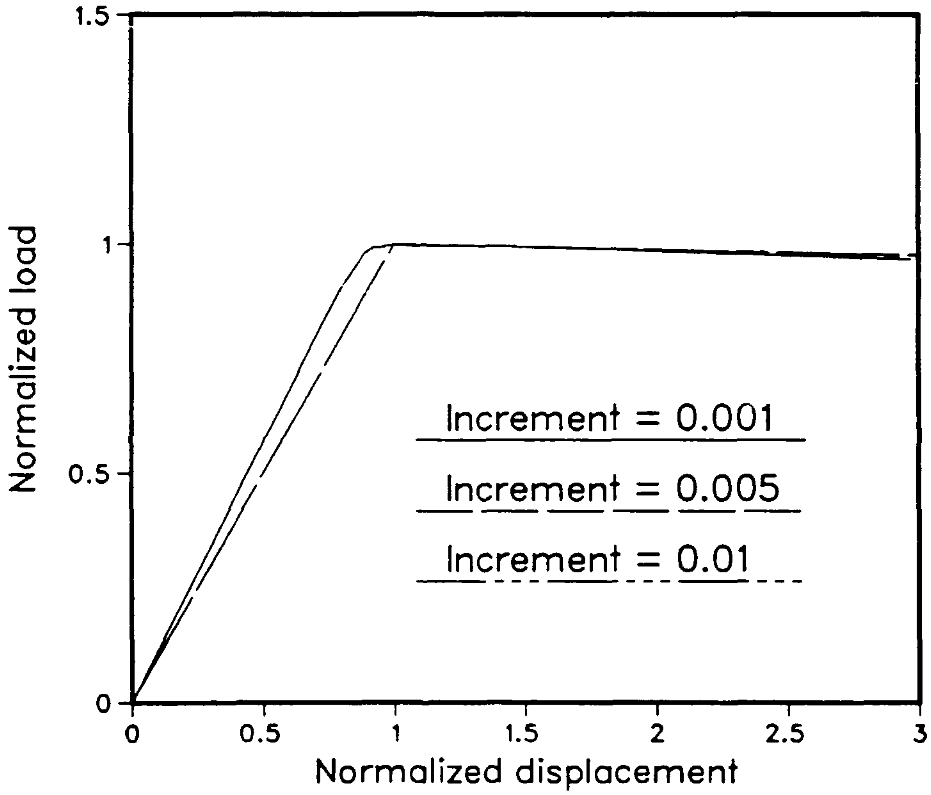

Figure 8. The effect of the size of prescribed total strain increments on numerical solutions.

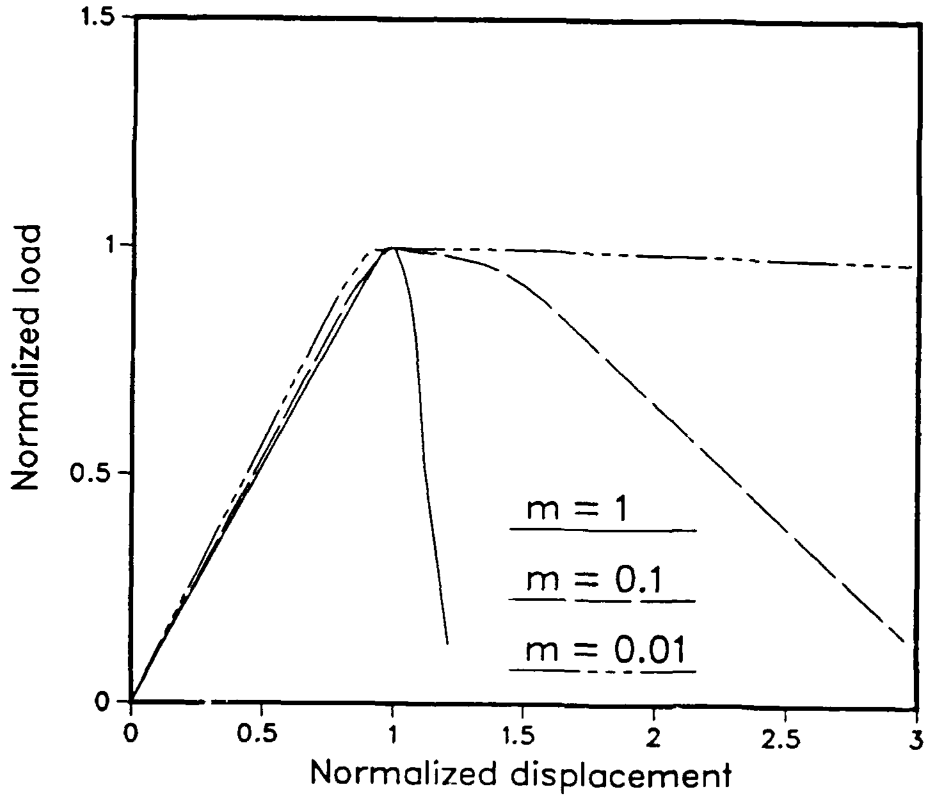

Figure 9. The effect of the softening parameter on load-displacement curves for plane strain.

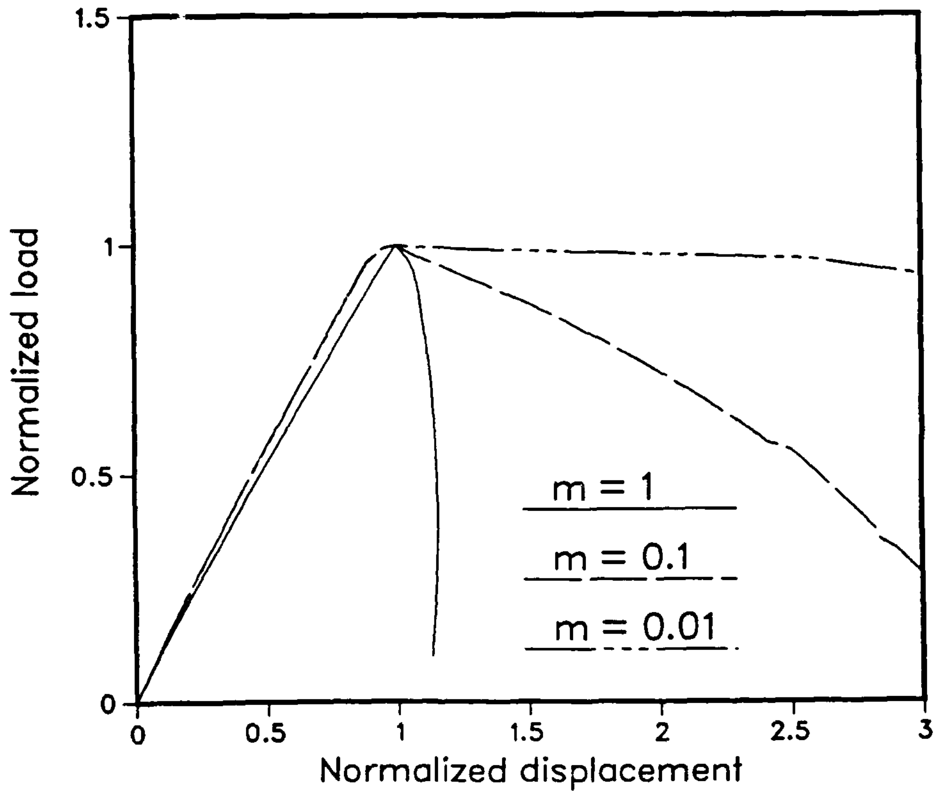

Figure 10. The effect of the softening parameter on load-displacement curves for plane stress.

ranging from almost perfect plasticity to a slight reversal where the post-peak response is taken down to a load that is close to zero. However, it must be emphasized that for this study nonlinear geometrical effects are not included, so that the potential problems discussed by de Borst (18), which are associated with mesh distortion and lockup, are precluded.

In monitoring the negative pivots in the $\mathbf{L}\text{-}\mathbf{D}\text{-}\mathbf{L}^T$ decomposition of the tangent stiffness matrix, it was noted that for the case of plane stress, negative pivots did not appear until those elements in the softening zone attained a high degree of softening. In other words, it seemed that the appearance of negative eigenvalues (immediate post-peak regime) was not accompanied by the appearance of negative pivots. Since this result is contrary to basic theory in matrix analysis, there must be an explanation involving round off and numerical accuracy. The results for plane strain are consistent with what might be expected from theory.

Because a local constitutive model is used, a mesh dependence is expected for the post-peak response. Such a dependence is shown in Figs. 11 and 12 for plane strain and plane stress with m = 0.1 and a prescribed strain increment of of 0.001. The need for nonlocal models to prevent this mesh dependency has been discussed by Schreyer and Chen (19), Chen and Schreyer (20), and Pijaudier-Cabot and Bazant (21), among others. Chen (22) has extended the above analysis procedure to show that the mesh dependency is significantly reduced for soil-structure interaction problems when a nonlocal constitutive model is used.

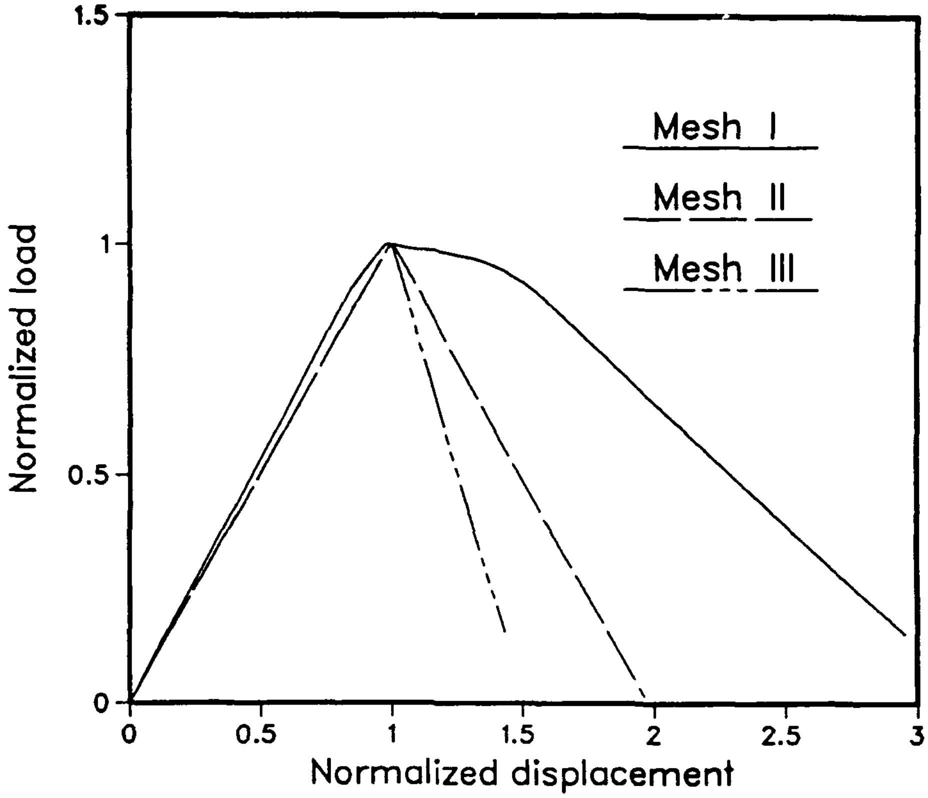

Figure 11. Illustration of mesh dependence for plane strain.

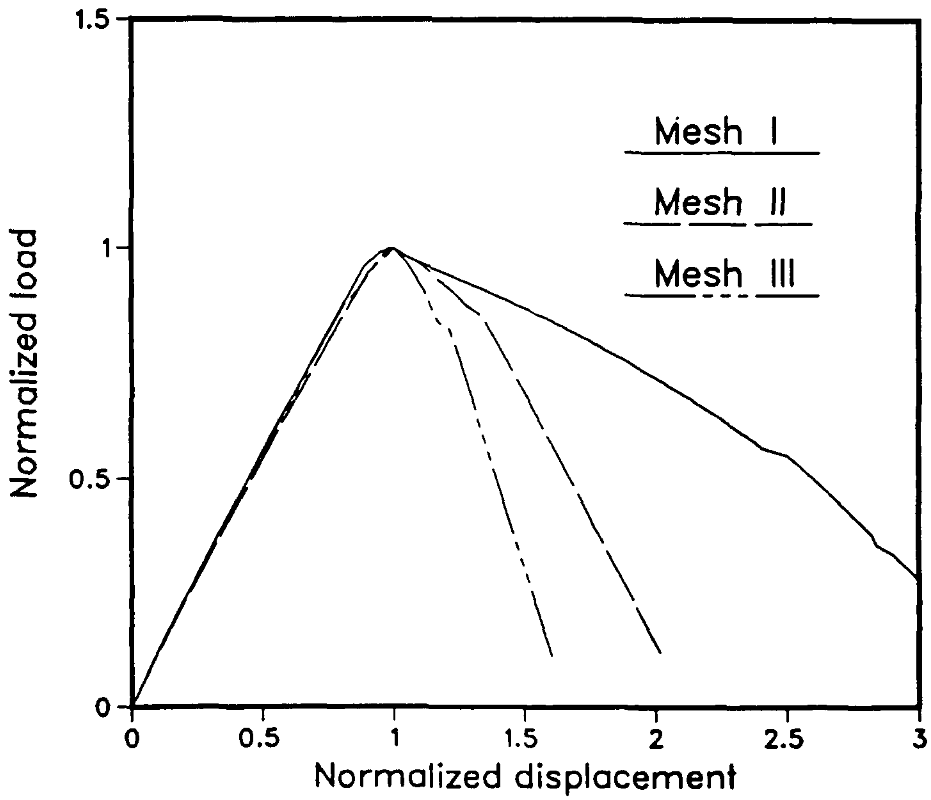

Figure 12. Illustration of mesh dependence for plane stress.

4.0 CONCLUSIONS

A slight modification to existing arc-control methods for obtaining numerical solutions to problems exhibiting post-peak softening is proposed in which a particular linear combination of the components of the total strain increment is prescribed at a critical point. There is no reason why the method could not be easily extended to include any norm of the total strain increment tensor. Then the load increment is automatically determined with the result that the procedure is particularly robust for transitioning critical points at which an eigenvalue of the tangent stiffness matrix is zero. The examples involve materially nonlinear problems, but the procedure should also be applicable to geometrically nonlinear cases.

The examples show that the evolution of failure modes is quite sensitive to the location of initial imperfections and to boundary conditions. Such results are in agreement with many experiments involving materials such as concrete where laboratories have reported significantly different failure loads and failure mechanisms for specimens composed of one batch of concrete. The current analysis indicates that such diversity may be entirely consistent with the slightly different boundary conditions associated with different experimental apparatuses.

REFERENCES

1. Bathe, K. J., **Finite Element Procedures in Engineering Analysis**, Prentice-Hall, Inc., Englewood Cliffs, NJ, 1982.

2. Shah, S. P. and Gopalaratnam, V. S., Softening response of plain concrete in direct tension. **J. of the American Concrete Institute**, 82, pp. 310-323, 1985.

3. Van Mier, J. G. M., **Strain-Softening of Concrete under Multiaxial Loading Condition**, PhD Dissertation, University of Einhoven, The Netherlands, 1984 (unpublished).

4. Belytschko, T. and Lasry, D., Localization limiters and numerical strategies for strain-softening materials. **Cracking and Damage: Strain Localization and Size Effect**, Proceedings of the France-US Workshop on "Strain Localization and Size Effect due to Cracking and Damage" held at the Laboratoire de Mecanique et Technologie, Cachan, France, 6-9 September 1988, edited by Mazars, J. and Bazant, Z. P., pp. 349-362, 1989.

5. Crisfield, M. A., A fast incremental/iterative solution procedure that handles "snap through." **Computers and Structures**, 13, pp. 55-62, 1981.

6. Ramm, E., Strategies for tracing non-linear responses near limit points. **Non-linear Finite Element Analysis in Structural Mechanics**, edited by Wunderlich, W., Stein , E., and Bathe, K. J., Springer-Verlag, New York, pp. 68-89, 1981.

7. Argyris, J. H., Continua and Discontinua. **Proceedings of 1st Conference in Matrix Methods in Structural Mechanics**, Wright-Patterson Air Force Base, Ohio, pp. 11-189, 1965.

8. Ramm, E., The Riks/Wempner approach--an extension of the displacement control method in nonlinear analyses. **Recent Advances in Non-Linear Computation Mechanics**, edited by Hinton, E., Owen, D. R. J., and Taylor, C., Swansea, U. K., pp. 63-86, 1982.

9. Padovan, J. and Tovichakchaikul, S., Self-adaptive predictor-corrector algorithms for static nonlinear structural analysis. **Computers and Structures**, 15, pp. 365-377, 1982.

10. de Borst, R., **Nonlinear Analysis of Frictional Materials**, PhD Dissertation, Delft University of Technology, Delft, The Netherlands, 1986.

11. Crisfield, M. A. and Wills, J., Solution strategies and softening materials. Personal communication, 1988.

12. de Borst, R., Computation of post-bifurcation and post-failure behavior of strain-softening solids. **Computers and Structures**, 25, pp. 211-224, 1987.

13. Crisfield, M. A., An arc-length method including line searches and accelerations. **International Journal for Numerical Methods in Engineering**, 19, pp. 1269-1289, 1983.

14. Golub, G. H. and van Loan, C. F., **Matrix Computations**, The Johns Hopkins University Press, Baltimore, Maryland, 1983.

15. Rots, J. G., **Computational Modeling of Concrete Fracture**, PhD Dissertation, Delft University of Technology, Delft, The Netherlands, 1988.

16. Nagtegaal, J. C. D., Parks, D. M., and Rice, J. R., On numerically accurate finite element solutions in the fully plastic range. **Computer Methods in Applied Mechanics and Engineering**, 4, pp. 153-177, 1974.

17. Leroy, Y., Needleman, A., and Ortiz, M., An overview of finite element methods for the analysis of strain localization. **Cracking and Damage, Strain Localization and Size Effect**, Proceedings of the France-US Workshop on "Strain Localization and Size Effect due to Cracking and Damage" held at the Laboratoire de Mecanique et Technologie, Cachan, France, 6-9 September 1988, edited by Mazars, J. and Bazant, Z. P., pp. 269-294, 1989.

18. de Borst, R., Analysis of spurious kinematic modes in finite element analysis of strain-softening solids. **Cracking and Damage, Strain Localization and Size Effect**, Proceedings of the France-US Workshop on "Strain Localization and Size Effect due to Cracking and Damage" held at the Laboratoire de Mecanique et Technologie, Cachan, France, 6-9 September 1988, edited by Mazars, J. and Bazant, Z. P., pp. 335-345, 1989.

19. Schreyer, H. L., and Chen, Z., One dimensional softening with localization. **Journal of Applied Mechanics, 53**, 791-797, 1986.

20. Chen, Z., and Schreyer, H. L., Simulation of soil-concrete interfaces with nonlocal constitutive models. **Journal of Engineering Mechanics**, 113, pp. 1665-1677, 1987.

21. G. Pijaudier-Cabot and Bazant, Z. P., Local and nonlocal models for strain-softening, and their comparison based on dynamic analysis. **Cracking and Damage, Strain Localization and Size Effect**. Proceedings of the France-US Workshop on "Strain Localization and Size Effect due to Cracking and Damage: held at the Laboratoire de Mecanique et Technologie, Cachan, France, 6-9 September 1988, Edited by Mazars, J. and Bazant, Z. P., pp. 379-390, 1989.

22. Chen, Z., **Nonlocal Theoretical and Numerical Investigations of Soil-Concrete Interfaces**, PhD Dissertation, University of New Mexico, Albuquerque, New Mexico, 1989.

DISTRIBUTION LIST

Dept of the Air Force

AUL/LSE Maxwell AFB, AL 36112	1 copy
HQ AU Attn: Tech Library Maxwell AFB, AL 36112-5001	1 copy
AF Institute of Technology/DE Attn: Tech Library Wright-Patterson AFB, OH 45433-5001	1 copy
FCDNA/FC Kirtland AFB, NM 87115-5000	1 copy
USAFA Attn: Tech Library Dept of Civil Engineering Colorado Springs, CO 80840-5001	1 copy
BMO/MYET Norton AFB, CA 92409-6468	1 copy
HQ AFESC Attn: Tech Library Tyndall AFB, FL 32402-6001	1 copy
HQ AFESC/RD Tyndall AFB, FL 32542-5000	1 copy
HQ AFSC/XTH Andrews AFB, MD 20334-5000	1 copy
HQ AFSC/DE Andrews AFB, MD 20334-5000	1 copy
HQ PACAF/DE Hickam AFB, HI 90853-5001	1 copy
HQ USAF/LEED Bolling AFB Washington DC 20330-5120	1 copy
Weapons Laboratory Attn: NT Kirtland AFB, NM 87117-6008	1 copy

DISTRIBUTION LIST (CONTINUED)

Weapons Laboratory Attn: NTE Kirtland AFB, NM 87117-6008	1 copy
Weapons Laboratory Attn: NTED Kirtland AFB, NM 87117-6008	1 copy
Weapons Laboratory Attn: NTEO Kirtland AFB, NM 87117-6008	1 copy
Weapons Laboratory Attn: NTES Kirtland AFB, NM 87117-6008	2 copies
Weapons Laboratory Attn: NTESG Kirtland AFB, NM 87117-6008	2 copies
Official Record Copy WL/NTESR (Maj John Gill) Kirtland AFB, NM 87117-6008	2 copies
Weapons Laboratory Attn: SUL Kirtland AFB, NM 87117-6008	2 copies
Weapons Laboratory Attn: HO Kirtland AFB, NM 87117-6008	2 copies

Dept of the Army

Harry Diamond Lab Attn: Library 2800 Powder Mill Road Adelphi, MD 20783	1 copy
US Army Engr Waterways Exper Sta Attn: Tech Library P.O. Box 631 Vicksburg, MS 39181	1 copy

DISTRIBUTION LIST (CONTINUED)

US Army Engr Waterways Exper Sta Attn: Dr Rohani P.O. Box 631 Vicksburg, MS 39181	1 copy
US Army Construction Engineering Research Laboratory Attn: Technical Library P.O. Box 4005 Champaign, IL 61820-1305	1 copy
US Army Corps of Engineers Omaha District MORED-ST 6014 USPO & Courthouse Omaha, NE 68102-4978	1 copy

Dept of the Navy

Naval Research Lab (NRL) Attn: Code 2627, Tech Lib Washington DC 20375	1 copy
Naval Surface Weapons Center Attn: Tech Library Dahlgren, VA 22448	1 copy
Naval Civil Engrg Lab Attn: Library (Code L08A) Port Hueneme, CA 92043	1 copy
Naval Surface Weapons Center White Oak Laboratory Attn: Code X221, Tech Library Silver Spring, MD 20910	1 copy

Government Agencies

Defense Nuclear Agency Attn: SPSD (Kent Goaring) Washington DC 20301	1 copy
DTIC/FDAC Cameron Station Alexandria, VA 22304-6145	2 copies

DISTRIBUTION LIST (CONCLUDED

Director Attn: SPSD (LTC Rubio) Defense Nuclear Agency Washington DC 20305-1000	1 copy

Government Contractors

AFELM Rand Corporation, Library D P.O. Box 2138 Santa Monica, CA 90406	1 copy
Sandia National Laboratories Attn: Tech Lib, Div 3141 Kirtland AFB, NM 87185	1 copy
University of New Mexico Attn: D. Calhoun NMERI P.O. Box 25, University Station Albuquerque, NM 87131	1 copy
Karagozian & Case Attn: John Karagozian 620 N. Brand Blvd #300 Glendale, CA 91203	1 copy